

Interactions of Solvents with Low Molar Mass and Side Chain Polymer Liquid Crystals Measured by Inverse Gas Chromatography

Ian M. Shillcock and Gareth J. Price*

Department of Chemistry, University of Bath, Claverton Down, Bath BA2 7AY, U.K.

Received: May 12, 2004; In Final Form: August 12, 2004

Inverse gas chromatographic measurements of infinite dilution Flory–Huggins interaction parameters, χ , as well as “hard-core” interaction parameters, χ^* , and energy exchange parameters, X_{12} , are reported for 17 nonpolar hydrocarbon solvents in various phases of hexyloxy- and octyloxycyanobiphenyl liquid crystals. The values are compared with those from a liquid crystalline siloxane polymer substituted with the cyanobiphenyl mesogen. The results are correlated with the structural features of the LC’s, and enthalpic and entropic contributions to the interactions are determined. The results suggest that interactions influenced by the mesogen are dominant, and the polymer backbone plays only a relatively minor part in the solution thermodynamics.

Introduction

Liquid crystal (LC) compounds have found a variety of uses and both low molar mass and polymeric versions have been developed into useful materials.^{1,2,3} Some applications, such as dyes, coatings, and films, utilize LC’s dissolved in a solvent or dispersed in a carrier polymer, and further development of these applications requires in-depth knowledge of the interactions between the components. A number of methods can be used to study structural features of LC systems.

Inverse gas chromatography, IGC, has been used to investigate the physicochemical properties of a wide range of systems including polymers.^{4,5} While it is a dynamic method, it was shown some years ago that measurements recorded under the correct conditions could give accurate equilibrium thermodynamic information.^{6,7} The retention of a solvent or “probe” molecule in the material is recorded, and the measurement made effectively at infinite dilution of the probe. A range of thermodynamic parameters can then be calculated.

Chow and Martire⁸ applied IGC to the study of a range of LC systems and developed a semiquantitative model which has been applied by several workers to describe the activity coefficients for homologous series of probe solvents in several LC systems.^{9–12} A number of attempts have been made to produce a more quantitative description of LC–solvent interactions but have added little to the ability to account for the observed behavior. For example, the model of Chow and Martire has been developed into a more rigorous statistical mechanical model based on a perturbation theory.¹³ Bocquet and Pommier¹⁴ extended the work to finite concentration and proposed a modified retention model. Coca and co-workers¹⁵ applied the classical Flory–Huggins theory to mesophases with nonmesogenic probes to account for the difference in sizes of the respective molecules. More recently, attempts have been made to combine the Maier–Saupe¹⁶ treatment of nematic LC’s with the Flory–Huggins theory to predict phase equilibrium in polymer–LC systems.^{17,18}

One of the most commonly used and studied LC systems is the alkyl- or alkoxy-substituted cyanobiphenyls which have been

widely used in display applications. Martire and co-workers,^{9,11} have studied a series of alkylcyanobiphenyls using IGC, characterizing them in terms of activity coefficients and the associated enthalpies and entropies associated with the solution process. In contrast, there have been only a few studies of LC polymers, particularly where the mesogen is attached to the polymer in a side chain^{19,20} or of main chain LC polymers where the mesogen is part of the backbone of the polymer.^{21,22} A comparison of the behavior of siloxane-substituted cyanobiphenyls with low molar mass equivalents has been reported²⁰ briefly by Price and Shillcock and the work described in this paper extends that study.

This paper presents work aimed at quantifying interactions in LC containing materials. In a previous publication²³ the behavior at infinite dilution of several systems was discussed in terms of the probe activity coefficients. In this paper, interaction parameters for two low molar mass alkoxybiphenyl LC’s and a side chain LC polymer bearing the same mesogen are reported and interpreted in terms of the chemical structures of the compounds involved.

Experimental Section

Materials. The liquid crystals studied were 4-(*n*-hexyloxy)-4'-cyanobiphenyl, HCB, 4-(*n*-octyloxy)-4'-cyanobiphenyl, OCB, and the polymeric poly(dimethyl-*co*-methyl(4-cyanobiphenoxy)-butyl siloxane), PDCBBS, which had 40 repeat units. They were all supplied by Merck(UK) Ltd. with reported purities of 99.5+%. The structures are shown in Figure 1 along with the transition temperatures and displayed mesophases reported by the manufacturers. The compounds were selected to display a range of mesophase behavior while retaining the same basic mesogen structure. In Figure 1 and the following discussion, Cr represents the solid, crystalline phase, N, the nematic mesophase, and SmA, the smectic-A mesophase. Poly(dimethylsiloxane), PDMS, was fractionated from a DC12500 fluid from Dow Corning and had a number-average molecular weight and polydispersity of 24100 and 3.8 respectively as measured by gel permeation chromatography. All probe solvents (Aldrich Chemicals or Merck Ltd.) were 99% pure or better. In this initial

* Corresponding author. Fax: + 44 1225 386231. E-mail: g.j.price@bath.ac.uk.

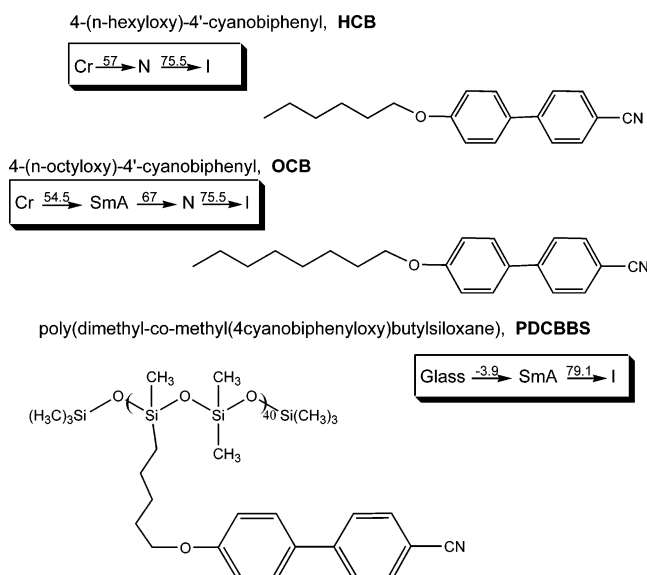


Figure 1. Structures and mesophase transition temperatures (°C) for the liquid crystals.

phase of work, study was confined to nonpolar probes to simplify the theoretical analysis.

Inverse Gas Chromatography. The stationary phases were prepared on acid washed, silanized Chromosorb P with 100–120 mesh size (Phase Separations). Coating was performed by slurrying the LC dissolved in the minimum amount of chloroform with the support followed by removal of the solvent under rotary evaporation. After drying, 1–1.5 m lengths of 1/4 in. o.d. copper tubing which had been washed successively with methanol, acetone, and toluene were packed with a known mass of the LC coated support with the aid of a water suction pump and mechanical vibrator. The column was loaded and conditioned for 24 h at 80 °C under a flow of carrier gas. The amount of LC or polymer on the support was determined by duplicate ashings on about 1 g of material or, for the siloxane materials, by exhaustive Soxhlet extractions of a similar amount of packing with chloroform, accounting for extractable matter from the uncoated support. For HCB and OCB, loadings of $14.3 \pm 0.2\%$ were used, the corresponding value for PDCBBS was $10.0 \pm 0.2\%$. Previous work²⁰ has shown that the support does not influence the behavior of the LC's at these loadings.

Measurements were performed on a Carlo Erba 400 chromatograph fitted with FID detectors using oxygen-free nitrogen as the carrier gas and modified to allow accurate measurement of the inlet and outlet pressures across the column. Gas flow rates in the range of 20–40 cm³ min⁻¹ were used, adjusted to give retention times with appropriate accuracy. Samples of ~0.01 μL of probe liquid and 0.4 μL of methane were injected from a 0.5 μL capacity Hamilton syringe. Where baseline separation was possible, several different probes were injected together. Retention times were recorded to ± 0.01 min on a Hewlett-Packard 3390A integrator. Each of the values reported is the mean of at least three measurements agreeing within $\pm 1\%$ of the net retention time. Estimation of the marker retention using methane or by extrapolation of the retention of consecutive *n*-alkanes were in close agreement. The column temperature was monitored to ± 0.1 °C using a thermocouple that had been calibrated against a Tinsley Type 5840 platinum resistance thermometer. The temperature variation through the oven was less than 0.2 °C. The usual checks⁵ were made to ensure that the results were independent of sample size and flow rate and that measurements were being made at infinite dilution.

Density Measurements. A method involving the displacement of water was employed. A glass displacement cell with ~5 cm³ capacity was made in-house, and the exact volume was determined by weighing the amount of triply distilled water held at 25.0 °C. About 1 g of material was placed into the cell, weighed, heated to the isotropic phase, and carefully frozen so that no air was trapped in the sample. The cell was filled with water and heated to the temperature of interest for 30 min and removed, quickly dried, and reweighed. Masses were accurate to ± 0.0005 g, and the temperature was constant to ± 0.01 °C. Results were obtained from at least two separate sets of measurements. From the difference in mass of the full cell, the density of the solid was determined. The density of the water used was determined using a ~10 cm³ density bottle with accurately known volume.

Results and Discussion

Data Treatment and Theory. The usual starting point for considering mixtures of components with very different sizes such as polymer solutions is the Flory–Huggins equation, eq 1, which accounts for the chemical potential, μ_1 , and activity of the solvent, a_1 in a solution in terms of the volume fractions, ϕ , of the solvent (probe), 1, and polymer (LC), 2, and the interaction parameter, χ .

$$\ln(a_1) = \frac{(\mu_1 - \mu_1^\circ)}{RT} = \ln(\phi_1) + \left[1 - \left(\frac{V_1^\circ}{V_2^\circ}\right)\right]\phi_2 + \chi\phi_2^2 \quad (1)$$

where V° is the molar volume of a component. In eq 1, the first two terms on the right-hand side account for the combinatorial entropy of mixing. The interaction parameter, χ , was originally introduced to account for enthalpic effects as the difference in interaction energies between polymer segments and solvent compared with those in the pure components. However, it is more correctly defined as a residual partial molar Gibbs free energy with both enthalpic (H) and entropic (S) contributions.

$$\chi = \chi^H + \chi^S \quad (2)$$

χ^S therefore corresponds to the noncombinatorial entropy of mixing. In addition, the interaction parameter has been found to be concentration dependent, usually fitted by a power series in ϕ_2 . These problems have recently been addressed by Wolf and co-workers.^{24,25} However, for IGC work, we are operating at infinite dilution and so it is not necessary to consider concentration variations.

In many cases, precise interpretation of χ is difficult and so it is commonly regarded as an empirical parameter which describes solvent quality in the solution.²⁶ The interaction parameter may be calculated from the specific retention volume, V_g° , of a probe in a chromatographic experiment (discussed in more detail below).

$$\chi^\infty = \ln\left(\frac{273.15Rv_2}{V_g^\circ p_1^\circ V_1^\circ}\right) - \left(\frac{p_1^\circ (B_{11} - V_1^\circ)}{RT}\right) - \left(1 - \frac{V_1^\circ}{V_2^\circ}\right) \quad (3)$$

where V_1° , B_{11} , and p_1° are respectively the molar volume, the second virial coefficient, and the saturated vapor pressure of the probe vapor at the column temperature T . M is the relative molar mass of a component.

In more recent work, the use of the volume fraction as a concentration variable in eq 1 has been replaced by a temperature independent “hard-core” volume which gives a better

representation of the fundamental size of a molecule on a lattice model and better quantification of the combinatorial entropy. Its introduction necessitates modification to eq 3 to calculate the interaction parameter on this basis, denoted χ^* :

$$\chi^* = \ln \left(\frac{273.15 R \nu_2^*}{V_1^* p_1^*} \right) - \left(\frac{p_1^* (B_{11} - V_1)}{RT} \right) - \left(1 - \frac{V_1^*}{M_2 \nu_2^*} \right) \quad (4)$$

In eq 4, V_1^* and ν_2^* represent the molar core volume of the probe liquid and the specific core volume of the polymer respectively, calculated from the thermal expansion coefficients of the materials. These values are available in the literature.²⁶

A major assumption in the Flory–Huggins treatment is that of zero volume of mixing and the use of temperature independent lattice site sizes. To overcome these problems and to give a more accurate description of fluid behavior, Flory, Orwoll, and Vrij developed an equation of state approach for polymer fluids. This used a reduced equation of state with parameters defined in terms of characteristic pressures, volumes, and temperatures. From this approach, it may be shown that the interaction parameter in eq 4 can be defined by

$$\mu_1^R = RT \phi_2^2 \chi^* = P_1^* V_1^* \left(\frac{1}{\tilde{\nu}_1} - \frac{1}{\tilde{\nu}} + 3 \tilde{T}_1 \ln \left(\frac{\tilde{\nu}_1^{1/3} - 1}{\tilde{\nu}^{1/3} - 1} \right) \right) + \frac{V_1^* \theta_2^2}{\tilde{\nu}_1} X_{12} \quad (5)$$

where μ_1^R is the residual or noncombinatorial chemical potential, V_1^* and ν^* are defined as above, P_1^* is the characteristic pressure used to calculate the reduced pressures. The first term in eq 5, where the tilde “ \sim ” signifies reduced quantities,²⁷ describes the entropic contribution to χ^* due to differences in thermal expansivity and free-volume between the components. The second term contains X_{12} , the “exchange interaction parameter” which characterizes the energetic interactions in terms of surface contact fractions, θ_2 between polymer and solvent.

This approach has been applied to a number of systems including solutions of polystyrene and PDMS with success. It is not though without problems; for example, the characteristic parameters should by definition be constant, but they were found to vary with temperature.²⁷ However, the FOV model offers a reasonable description of the solution while requiring only a small number of measured parameters. A development of the model was suggested²⁷ by the introduction of a correction term, Q_{12}

$$X_{12}^m = X_{12} - Q_{12} \tilde{\nu} T \quad (6)$$

where X_{12} is the exchange interaction parameter and superscript m denotes the measured value. This is analogous to introducing the χ^S term in eq 2 by introducing an entropic contribution into the interaction term. Both positive and negative values of Q_{12} have been reported in other systems making interpretation of the precise significance of the term difficult and it may be used as an empirical measure of the degree of ordering imposed within a solution.

In considering systems involving liquid crystals, the anisotropic arrangement of the molecules must also be taken into account. The most used model for LC fluids is the Maier and Saupe^{3,16} treatment using a mean field approximation applied to rigid rod nematic phases. The approach has been used with reasonable success to determine order parameters as a function

of temperature and to predict nematic to isotropic transitions. However, the work described here is primarily concerned with the effect the anisotropy of the LC has upon an absorbed probe molecule and so this model is not directly applicable. Martire and Yan^{13,28} considered the absorption of a solvent into the nematic and isotropic phases of a LC and derived expressions for the chemical potentials of a probe molecule. However, application requires detailed knowledge of the molecular dimensions of both the rigid core of the LC and the flexible groups as well as an estimate of the energy required to deform the flexible chain. A number of secondary parameters defining the order within the solution must be calculated, and hence application of the model is limited. Brostow and co-workers^{29,30} have also provided a description of phase behavior of mixtures including LC's in reasonable agreement with experimental observations.

Flory and co-workers approached the problem by considering the mixing of rigid polymer components with orientation-dependent interactions.³¹ Semiquantitative agreement with the observed phase behavior in a number of systems was demonstrated.³² The basis of the treatment is that the anisotropic nature of the mesophase is governed predominantly by the molecular shape and size of the components with the interactions between molecules contributing a perturbation to the mixture. The general lattice model is modified by two extra parameters, η and y ; the first denoting the number of lattice segments in a rigid sequence, obtainable from the molecular structure. The second term, y , is the “disorientation parameter” related to how many lattice sites are needed to accommodate the oriented mesogenic sequence. In this case, the activity of the solvent in an anisotropic phase is given by (cf. eq 1 for the isotropic case)

$$\ln(a_1) =$$

$$\ln(\phi_1) + \left[1 - \left(\frac{V_1^*}{V_2^*} \right) \right] \phi_2 + \left(\frac{2}{y} \right) + \left(1 - \exp \left(\frac{-2}{y} \right) \right) + \chi \phi_2^2 \quad (7)$$

Flory showed that η is independent of y and only depends on the proportion of the rigid sequences of the polymer that are aligned, i.e., the effective degree of alignment in the LC. At equilibrium, y can be calculated from

$$\exp \left(\frac{-2}{y} \right) = 1 - \phi_o^a \left(1 - \frac{y}{\eta^a} \right) \quad (8)$$

where ϕ_o^a is the volume fraction of aligned, rigid sequences in the LC and η^a is the average number of segments in the aligned portions of the polymer chain. The theory does not specify a particular type of anisotropic ordering, although a nematic mesophase is often implicitly assumed.

Densities of the LC's. To calculate V_2^* and ν_2 , the densities of the polymer and LC's are needed. To ensure the validity of the experimental method used, the densities of a polystyrene sample (1.084 g cm⁻³ at 25 °C) and of the PDMS used in the thermodynamic measurements (0.9713, 0.9508, and 0.9394 g cm⁻³ at 25, 46.5, and 58.5 °C respectively) were measured and were in excellent (<1% difference) agreement with literature³³ results. The results for the three LC's are shown in Figure 2, and it is apparent that the coefficient of expansion is higher in the isotropic phase. Linear fits to the results within each mesophase are listed in Table 1. Higher order analysis of the results did not significantly improve the fit of the data.

There was a small change in density at the mesophase transition temperatures, within the uncertainty in the measurements. However, the crystalline to mesophase transitions were

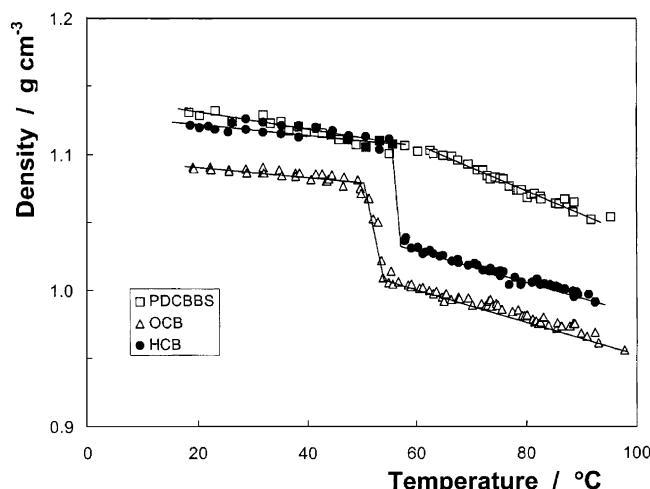


Figure 2. Temperature dependence of the densities of the liquid crystals.

TABLE 1: Linear Equations Describing Density (g cm^{-3}) as a Function of Temperature, T , in $^{\circ}\text{C}$ ^a

	phase	equation	σ
HCB	Cr	$1.140 - 5.53 \times 10^{-4}T$	0.005
	N	$1.107 - 1.267 \times 10^{-3}T$	0.003
	I	$1.080 - 9.30 \times 10^{-4}T$	0.004
OCB	Cr	$1.103 - 4.76 \times 10^{-4}T$	0.005
	SmA	$1.079 - 1.270 \times 10^{-3}T$	0.002
	N	$1.075 - 1.145 \times 10^{-3}T$	0.002
	I	$1.064 - 1.029 \times 10^{-3}T$	0.003
PDCBBS	SmA	$1.149 - 7.82 \times 10^{-4}T$	0.004
	I	$1.186 - 1.412 \times 10^{-3}T$	0.004

^a σ is the standard deviation of the line.

accompanied by a decrease in density of around 10%, and the transition temperatures could be obtained. In HCB, the change was very abrupt and occurred between 55.5 and 56.4 $^{\circ}\text{C}$. OCB had a broader change with the density decreasing between 49.6 and 53.6 $^{\circ}\text{C}$. If the transition temperature is taken as the higher temperature—the point where no more crystalline phase exists—these values are in agreement with those reported from the DSC measurements. OCB seems therefore to be exhibiting a small premelting transition. This phenomenon is well-known and has been noted in the crystal–mesophase and higher temperature mesophase transitions³⁴ of cholesteric liquid crystals. The transition is less marked in the polymer and there is more curvature in the plots, probably related to the polydispersity in the chain lengths.

Flory–Huggins Interaction Parameters. The primary datum in IGC is the specific retention volume, V_{g}° , the volume of carrier gas at STP per gram of stationary phase required to elute the probe.³⁵ This is related to the probe retention time, t_{R} , by

$$V_{\text{g}}^{\circ} = \frac{(t_{\text{R}} - t_{\text{M}})F'J}{W} \quad (9)$$

where t_{M} is the retention time of the methane marker, F' is the carrier flow rate corrected to STP, J is the correction for gas compressibility, and W is the mass of stationary phase on the column. F' was calculated from the measured flow rate, F , obtained under laboratory conditions and corrected for the laboratory temperature, T , and atmospheric pressure, p_{A} as well

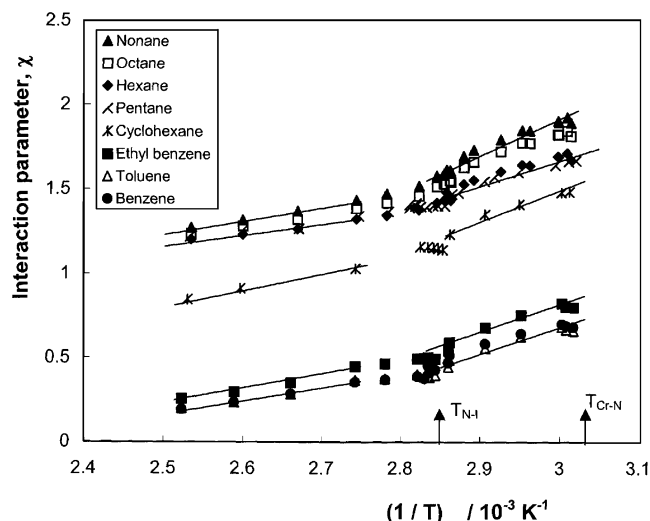


Figure 3. Flory–Huggins interaction parameters for probe solvents in HCB.

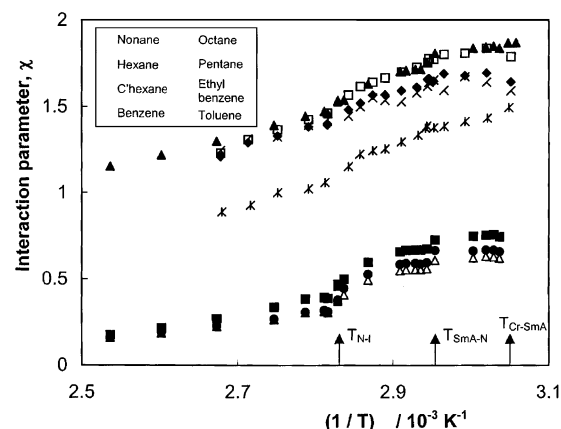


Figure 4. Flory–Huggins interaction parameters for probe solvents in OCB.

as for water vapor pressure, p_{w} in the flow-meter using literature constants.³⁶

$$F' = F \left(\frac{273.15}{T} \right) \left(\frac{760}{p_{\text{o}}} \right) \left[1 - \left(\frac{p_{\text{w}}}{p_{\text{A}}} \right) \right] \quad (10)$$

The correction factor for gas compressibility is given in terms of the column inlet and outlet pressures, p_{i} and p_{o} respectively by³⁷

$$J = \frac{3}{2} \left[\frac{(p_{\text{i}}/p_{\text{o}})^2 - 1}{(p_{\text{i}}/p_{\text{o}})^3 - 1} \right] \quad (11)$$

V_{g}° values were used to calculate³⁸ interaction parameters according to eqs 3 and 4. In calculating the interaction parameters reported below, pure component data were taken from reliable literature sources.^{39,36,40,41}

Low Molar Mass LC's. Figures 3 and 4 illustrate the temperature dependence of the χ parameters for a selection of the probes in the two low molar mass liquid crystals, HCB and OCB. The equivalent plots of χ^* gave the same features except for a small, consistent shift on the χ axis with χ^* generally being 0.01–0.1 higher. The uncertainty in the V_{g}° values was 1–1.5% and that in χ and χ^* was ± 3 –5%. Table 2 lists the interaction parameters (volume and hard-core versions) at a given temperature within the N and I phases of HCB and Table

TABLE 2: Flory–Huggins Interaction Parameters and Hard-Core Interaction Parameters at 68 °C in the Nematic Mesophase and at 86 °C in the Isotropic Liquid of HCB

probe	nematic, 86 °C		isotropic, 68 °C	
	χ^∞	χ^*	χ^∞	χ^*
pentane	1.58	1.65	1.37	1.44
hexane	1.61	1.65	1.35	1.43
heptane	1.68	1.69	1.39	1.44
octane	1.73	1.74	1.42	1.46
nonane	1.80	1.80	1.48	1.51
2-methylhexane	1.75	1.79	1.50	1.55
3-methylhexane	1.78	1.77	1.46	1.52
2,3-dimethylpentane	1.70	1.72	1.41	1.47
2,4-dimethylpentane	1.84	1.87	1.53	1.60
2,2,3-trimethylbutane	1.73	1.75	1.42	1.49
cyclohexane	1.40	1.40	1.10	1.16
benzene	0.62	0.63	0.37	0.48
toluene	0.59	0.59	0.38	0.43
ethylbenzene	0.72	0.71	0.47	0.50
<i>p</i> -xylene	0.56	0.55	0.36	0.39
<i>m</i> -xylene	0.63	0.62	0.43	0.46
<i>o</i> -xylene	0.58	0.57	0.35	0.38

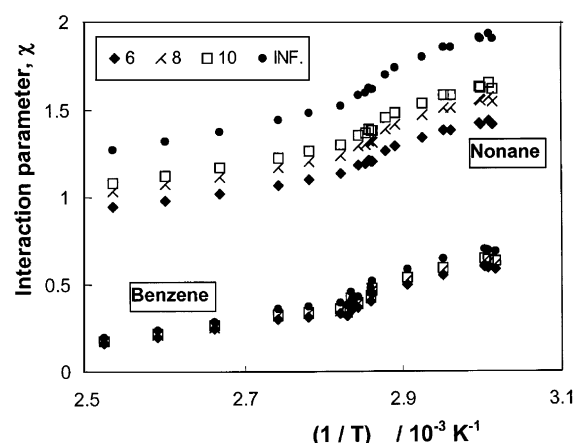
TABLE 3: Flory–Huggins Interaction Parameters and Hard-Core Interaction Parameters at 58 °C in the Smectic Mesophase, at 75 °C in the Nematic Mesophase, and at 90 °C in the Isotropic Phase of OCB

probe	smectic A, 58 °C		nematic, 75 °C		isotropic, 90 °C	
	χ^∞	χ^*	χ^∞	χ^*	χ^∞	χ^*
pentane	1.65	1.70	1.56	1.63	1.33	1.43
hexane	1.70	1.73	1.57	1.62	1.33	1.40
heptane	1.78	1.78	1.61	1.63	1.36	1.40
octane	1.84	1.84	1.65	1.66	1.37	1.40
nonane	1.85	1.84	1.64	1.65	1.41	1.43
2-methylhexane	1.62	1.63	1.42	1.45	1.18	1.23
3-methylhexane	1.60	1.61	1.39	1.42	1.14	1.20
2,3-dimethylpentane	1.56	1.58	1.37	1.40	1.10	1.15
2,4-dimethylpentane	1.63	1.65	1.45	1.49	1.20	1.26
2,2,3-trimethylbutane	1.55	1.56	1.35	1.39	1.12	1.16
cyclohexane	1.44	1.45	1.25	1.28	1.00	1.05
benzene	0.67	0.68	0.54	0.57	0.28	0.37
toluene	0.56	0.63	0.50	0.51	0.27	0.31
ethylbenzene	0.76	0.74	0.61	0.60	0.35	0.25
<i>p</i> -xylene	0.58	0.57	0.46	0.46	0.24	0.26
<i>m</i> -xylene	0.70	0.68	0.53	0.53	0.24	0.26
<i>o</i> -xylene	0.62	0.60	0.48	0.47	0.23	0.24

3 lists the corresponding results in the SmA, N and I phases of OCB. The arrows indicate the transition temperatures measured by DSC.

The plots in Figures 3 and 4 all have positive slopes indicating that mixing is endothermic. The values for the alkane probes are generally considerably higher than for the aromatics indicating that the latter are more compatible with the LC compounds. This suggests that the major source of the interaction is with the aromatic mesogen of the LC rather than with the alkyl chain. The values for a particular probe in each of the LC mesophases are similar, reinforcing this suggestion. χ and χ^* increase with increasing chain length of the alkane probe indicating decreasing compatibility. Values for the branched alkanes are also higher than the linear isomers. Previous consideration²³ of the enthalpies and entropies of solution for these systems suggested that the longer chain alkane probes are able to undergo stronger interactions with the liquid crystal but suffer from a greater constraint in the conformations they can adopt and that the branched isomers interact more weakly and are subject to lesser restriction on mobility in the mesophases.

The break in the plots at each of the mesophase transitions is readily apparent although there is scatter in the results around

**Figure 5.** Effect of number of end group neighbors on Flory–Huggins interaction parameters for nonane and benzene in HCB calculated assuming $z = 6, 8, 10$, and ∞ .

the transitions. Given the relatively small alteration in the molecular alignment during a mesophase transition in the stationary phase, this is an indication of the ability of the IGC method to investigate small changes in structure. The change in values takes place over a 1–2 °C across the range of probes used. The interaction parameters are seen to have a linear dependence on reciprocal temperature in each of the mesophases as expected from a free energy parameter and can be fitted to

$$\chi = b - \frac{a}{T} \quad (12)$$

In general, the nematic phase exhibits the larger temperature dependence and the smectic phase the least, consistent with the activity coefficient and enthalpy of mixing data reported previously.²³ In the smectic phase of OCB the aromatic probes exhibited significantly lower temperature dependence of χ than the aliphatics. The aromatics would be expected to favor interaction with the biphenyl rings which will largely be aligned in ordered layers and thus be more confined. They may therefore be less susceptible to thermal disruption, so lowering the temperature sensitivity.

When discussing these results, consideration needs to be given to the applicability of the Flory–Huggins approach in dealing with low mass materials. The combinatorial entropy contribution conforms to the same expression from a lattice theory. However, the free energy term arising from the interaction between segments on a lattice could require modification as a result of the increased influence of end groups. The end groups on the polymer are generally considered to be insignificant in polymer solutions but they will become more important when considering low molar mass materials. Inclusion of end group effects yields eq 12 for the activity coefficient at infinite dilution; ignoring end group effects leads to neglect of the final term.

$$\ln(\gamma_1^\infty) = \ln\left(\frac{V_2^\circ}{V_1^\circ}\right) + \left[1 - \left(\frac{V_1^\circ}{V_2^\circ}\right)\right] + \chi^\infty + 2\chi^\infty\left(\frac{V_1^\circ}{V_2^\circ(z-2)}\right) \quad (13)$$

where z is the number of first neighbor cells on the lattice. In a real fluid, the number of nearest neighbors is around 6–10.

This effect will be most marked for HCB because it was the smaller of the LC's studied. Figure 5 shows the effect of different z values on the interaction parameters for benzene and nonane in HCB. Ignoring the effect of end groups has a significant effect on χ . However, the trends in the values are the same for a given value of z . The effect is magnified for

TABLE 4: Interaction Parameters at Three Temperatures in HCB and OCB

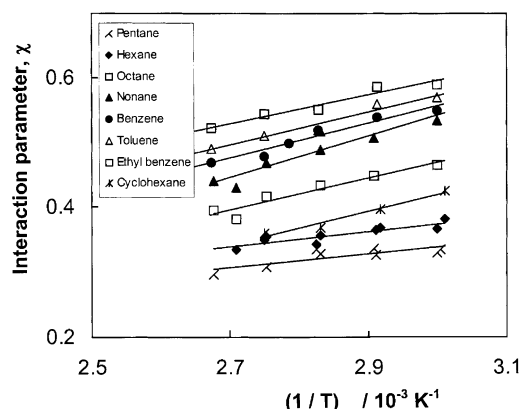
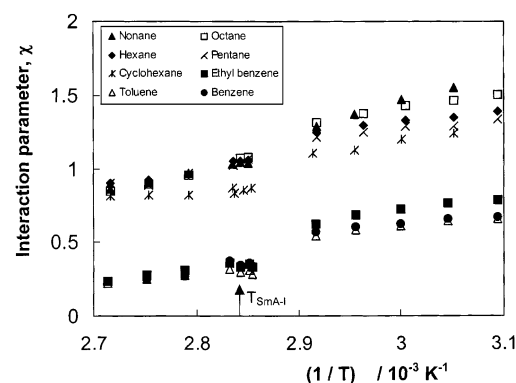
probe	97 °C		84 °C		72 °C	
	HCB	OCB	HCB	OCB	HCB	OCB
pentane	1.29	1.30	1.40	1.39	1.52	1.55
hexane	1.27	1.28	1.37	1.37	1.53	1.59
heptane	1.29	1.30	1.40	1.41	1.62	1.65
octane	1.34	1.30	1.42	1.43	1.66	1.69
nonane	1.40	1.35	1.48	1.46	1.75	1.70
cyclohexane	1.00	0.94	1.10	1.04	1.33	1.29
benzene	0.30	0.23	0.40	0.29	0.58	0.56
toluene	0.32	0.23	0.42	0.29	0.54	0.52
ethylbenzene	0.38	0.31	0.50	0.38	0.68	0.64

large values of χ and thus is more important for nonane than benzene. As a liquid crystal can form semioordered fluid phases, the number of first neighbor cells is likely to be closer to 10 than 6. As the z values are not known with certainty for the LC's used here, any correction to the measured values would be somewhat arbitrary, and while we note these possible complications, the assumption of an infinite value for z will be adopted in order to discuss the trends.

OCB contains two more methylene units in the alkyl chain than HCB. Table 4 lists the interaction parameters for some of the probes with HCB and OCB at temperatures where each exhibits isotropic and nematic phases. Note that the uncertainty in the measured values of χ was ± 0.04 . In the N phase (72 °C), the values of χ agree within experimental uncertainty for the two probes. The same is true for the alkane probes in the isotropic liquids above their clearing points. However, the aromatic probes have a somewhat stronger interaction (lower χ) with OCB. The same trends hold when considering χ^* .

To quantify this effect in a related system, interaction parameters for octadecane and hexadecane, also differing by two methylene groups, at 30 and 40 °C were calculated using the activity coefficient data of Laub et al.⁴² The values showed a consistent difference between these two compounds of 0.17–0.20 for the probes used in the work reported here, the results for octadecane being the larger. This is significantly larger than that observed for OCB and HCB and is consistent with the rigid biphenyl portion of the molecules governing the interactions with the probes, particularly in the mesophase where the additional order and enhanced interaction between adjacent mesogens is detrimental to the biphenyl–alkane interactions. That there is not a large increase in values for nematic OCB is indicative that there is some interaction with the alkyl chain despite it not being the dominant factor. The greater reduction in values for aromatic probes in the isotropic phase arises from the increased importance of the alkyl chain once the order of the liquid crystal has been removed.

The “hard-core” interaction parameters parameters are also listed in the tables above. Generally the trends and behavior are very similar to the classical interaction parameters already discussed. The main differences are that the alkane probes exhibit a smaller range of values at a given temperature and the benzene values are higher than toluene and ethylbenzene, resulting in a reversal of the trend with the aromatic probes. These changes are a consequence of the different rates of expansion of the probes. As the interaction parameter now accounts for all noncombinatorial entropy effects the values are higher than in the classical theory. As end groups will have a higher free-volume, the probes with the greater relative proportion of end groups, i.e., the lower n -alkanes and branched alkanes, will experience larger increases in χ . Thus, the alkane values occur over a narrower range.

**Figure 6.** Flory–Huggins interaction parameters for probe solvents in PDMS.**Figure 7.** Flory–Huggins interaction parameters for probe solvents in PDCBBS.

Polymer Systems. We then turned our attention to polymeric systems. Before considering the LC polymer, it is appropriate to consider the interactions with the siloxane backbone. Although there are several reports on PDMS systems in the literature, studied both by IGC and static methods, there is a wide variation in reported results and only a few give results at temperatures comparable with the present work. However, agreement with published work^{43–45} where appropriate was generally satisfactory considering the expected uncertainty of ± 0.02 – 0.04 in χ .

Interaction parameters calculated from our measurements are shown as a function of temperature in Figure 6. All gave the linear relation with reciprocal temperature expected for a polymer well above its glass transition. The values for aliphatic probe–PDMS systems are significantly lower than with the aromatic systems indicating better compatibility. The interaction parameters exhibited little temperature dependence for the probes studied.

Figure 7 shows the same plot for the liquid crystal polymer, PDCBBS, and the larger variation in results is readily apparent. The differences between the mesophase and the isotropic liquid are clear, the smectic phase giving much larger differences between the various probes. Indeed, the results for all four alkanes are virtually superimposable in the isotropic liquid and those for the aromatics are also very similar to each other. There is a difference in interaction between the alkanes and aromatics, with the latter interacting more favorably that is much more characteristic of the low molar mass LC's than of the polysiloxane.

Table 5 lists the interaction parameters for PDCBBS and OCB at a temperature where they both form a SmA mesophase and compares the values with those of PDMS at the same temper-

TABLE 5: Interaction Parameters, Hard-Core Interaction Parameters, for PDCBBS and Interaction Parameters for PDMS and OCB

probe	70 °C				85 °C			
	PDCBBS, SmA		PDMS	OCB, SmA	PDCBBS, I		χ PDMS	OCB, I
	χ	χ^*			χ	χ^*		
pentane	1.22	1.40	0.34	1.53	0.97	1.09	0.32	1.40
hexane	1.25	1.39	0.37	1.60	0.96	1.04	0.35	1.39
heptane	1.29	1.40	0.40	1.65	0.98	1.02	0.38	1.41
octane	1.31	1.41	0.45	1.70	0.95	0.98	0.44	1.43
nonane	1.29	1.37	0.51	1.71	0.97	0.98	0.50	1.45
2-methylhexane	1.27	1.38	0.37	1.48	0.98	1.03	0.36	1.22
3-methylhexane	1.27	1.39	0.37	1.46	0.95	1.00	0.35	1.19
2,3-dimethylpentane	1.21	1.33	0.33	1.42	0.92	0.98	0.31	1.16
2,4-dimethylpentane	1.30	1.44	0.34	1.49	1.02	1.10	0.32	1.26
2,2,3-trimethylbutane	1.19	1.32	0.29	1.41	0.92	0.98	0.27	1.16
cyclohexane	1.10	1.21	0.40	1.30	0.82	0.86	0.36	1.03
benzene	0.57	0.68	0.54	0.59	0.27	0.40	0.44	0.31
toluene	0.54	0.62	0.56	0.55	0.28	0.29	0.52	0.31
ethylbenzene	0.62	0.69	0.59	0.66	0.31	0.30	0.55	0.39
<i>p</i> -xylene	0.43	0.47	0.66	0.50	0.22	0.21	0.62	0.27
<i>m</i> -xylene	0.57	0.64	0.70	0.57	0.24	0.23	0.66	0.30
<i>o</i> -xylene	0.52	0.57	0.73	0.53	0.21	0.19	0.70	0.27

TABLE 6: Enthalpic and Entropic Contributions to the Interaction Parameter for Hexane and Benzene at Different Temperatures

phase	temp °C	hexane		benzene	
		χ^H	χ^S	χ^H	χ^S
PDMS	80.0	0.02	0.36	0.26	0.19
PDCBBS SmA	60.0	0.45	0.88	0.02	0.60
PDCBBS I	85.0	0.51	0.45	0.00	0.27
HCB N	66.0	0.74	0.91	0.00	0.65
HCB I	86.0	0.72	0.63	0.01	0.36
OCB SmA	58.0	0.68	1.02	0.00	0.67
OCB N	70.0	0.66	0.94	0.00	0.59
OCB I	85.0	0.78	0.61	0.02	0.29

ature. A similar comparison for the isotropic phase is also included. HCB does not form a SmA phase and so is not directly comparable. The values for PDCBBS are higher for aliphatic probes than for aromatic probes. This implies that the PDCBBS—probe solution is mainly governed by the mesogen both in the mesophase and the isotropic phase. However, the PDMS backbone exerts greater influence in the isotropic phase, which is evident from the greater similarity of the alkane probes in the isotropic phase.

To gain a measure of the relative contributions to the interactions, the enthalpic contribution to the overall interaction parameter, χ^H , can be calculated from

$$\chi^H = -T \left(\frac{d\chi^*}{dT} \right) \quad (14)$$

with χ^S then calculated from eq 2. As an example of the results, Table 6 shows the values for hexane and benzene in each of the LC mesophases and in PDMS. It is again apparent that the values in the LC polymer are much closer to those in the LC's than in the polysiloxane. In particular, the enthalpic contributions are very small for benzene with the aromatic LC's and the interaction is dominated by the entropy. Both elements contribute to the interaction in PDMS. This situation is reversed with hexane as the probe.

This discussion of the thermodynamic properties of these systems in terms of interaction parameters corroborates the conclusions previously made from a qualitative discussion of activity coefficient data.²³ However, the model also suggests that the observed behavior is governed mainly by the rigid mesogen and only moderated by the presence of the flexible

alkoxy end groups of these cyanobiphenyls. Hence, OCB and HCB exhibited similar interaction parameters for the same probe in the same type of mesophase at identical temperature. The polymeric liquid crystal also exhibited behavior suggesting that the mesogen governed the probe—LC interaction although the polymer backbone exerted a greater influence on the results than the flexible alkyl chains in the low molar mass cyanobiphenyls.

Anisotropy Effects on the Interaction Parameters. The interaction parameters should be unaffected by anisotropy in the isotropic phase. However from eq 7, in a mesophase the true interaction parameter, χ^T , is related to the measured value, χ , by³¹

$$\chi^T = \chi + (2/y) - (1 - \exp(-2/y)) \quad (15)$$

where y represents the number of adjacent rows in a lattice required to accommodate the aligned rigid mesogen and accounts for the anisotropy. Since y should be a constant value, any correction would result in a consistent shift for all probes. The trends in χ between different probes would remain the same, although the temperature dependence in the mesophases would change.

Using estimates of the length of the rigid mesogen, $\bar{\eta}^a$, and the volume fraction of aligned mesogens, ϕ_o^a , estimates of y can be obtained from eq 8 by solving

$$f(y) = \exp(-2/y) - 1 + \phi_o^a(1 - (y/\bar{\eta}^a)) = 0 \quad (16)$$

The value of y should strictly be an integer but can be treated⁴⁶ as a continually varying parameter. A system such as a cyanobiphenyl with benzene as the probe would be expected to fit this model closely. From the molecular dimensions of the cyanobiphenyls used here, three segments are required to accommodate the mesogen. In related work,⁴⁷ the degree of crystallinity of the mesophases in HCB and OCB has been estimated using IGC measurements and lay between 0.1 and 0.2 close to the melting temperatures, although this probably underestimates the true value. Using $\phi_o^a = 0.2$ and taking the size of a lattice segment as a cube of side equal to the diameter of the mesogen, we applied eq 16. However, there were no solutions at any concentration; indeed, no solution was found for any physically realistic value of the axial ratio, implying that the cyanobiphenyl mesogen is not long enough to require

TABLE 7: Exchange Interaction Parameters X_{12} (J cm^{-3}) for Hydrocarbons in LC Phases

probe	HCB		OCB		PDMS		PDCBBS	
	N 68	I 86	SmA 58	N 75	I 90	90	SmA 70	I 85
pentane	68.9	63.5	69.8	66.5	54.9	9.6	40.3	45.4
hexane	61.0	43.2	62.5	58.9	49.0	10.9	37.3	39.4
heptane	55.1	39.6	56.6	52.7	43.9	10.9	34.1	34.6
octane	51.3	37.3	52.7	48.7	40.4	11.7	31.9	30.3
nonane	48.1	35.6	47.5	44.0	37.7	12.1	28.5	27.5
2-methylhexane	58.2	44.4	51.7	46.9	38.7	10.9	35.1	35.1
3-methylhexane	58.2	42.7	52.1	46.4	37.4	10.0	34.6	34.3
2,3-dimethylpentane	57.3	41.7	51.4	46.0	36.4	9.6	33.3	33.8
2,4-dimethylpentane	60.5	43.8	52.5	47.3	38.3	8.8	34.7	36.5
2,2,3-trimethylbutane	58.2	42.2	50.8	45.4	39.9	8.4	32.9	33.6
cyclohexane	62.0	42.6	62.4	55.8	44.2	14.6	39.9	39.4
benzene	33.7	16.5	35.5	29.1	16.4	25.9	22.2	22.6
toluene	26.4	13.2	27.1	22.6	11.8	23.0	18.7	13.4
ethylbenzene	26.9	15.9	26.9	23.3	9.1	21.7	20.2	12.1
<i>p</i> -xylene	21.1	11.0	20.8	17.5	9.0	23.4	13.7	8.6
<i>m</i> -xylene	23.4	14.3	24.4	20.4	9.3	25.5	18.3	9.3
<i>o</i> -xylene	21.8	11.6	22.0	18.5	9.1	27.2	16.7	7.8

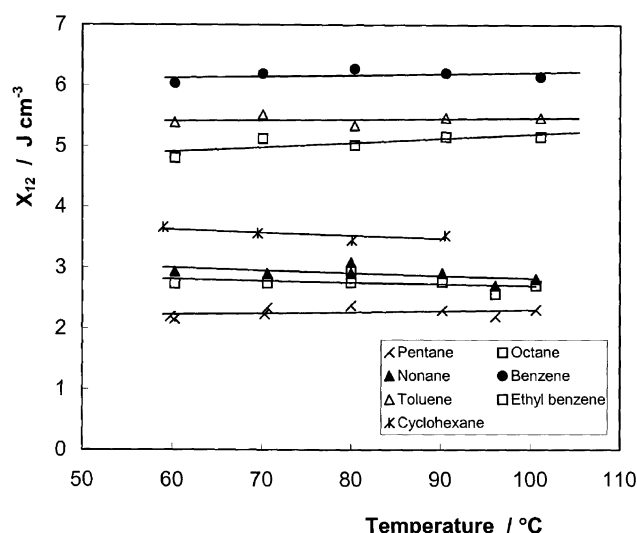


Figure 8. Energy exchange interaction parameters for probe solvents in PDMS.

correction to the calculated interaction parameters. Thus, according to this model, the mesophases of the cyanobiphenyls are sufficiently disordered for the anisotropy of the molecules to have an insignificant effect on the interaction parameters. As the disorientation parameter was introduced to describe the placement of LC's on a lattice, this does not imply that the anisotropy has no effect on the interactions but that a more refined description of the solution behavior than the Flory–Huggins theory would need to be employed before the anisotropy of small mesogens needs to be explicitly considered.

Equation of State Theory. The values of the exchange interaction parameters for the systems studied are shown in Table 7. The pure component data used to calculate the characteristic parameters were taken from literature constants.⁴⁸ In principle, the values should be independent of temperature although this has rarely been reported, leading to the use of eq 6. Figure 8 shows the X_{12} parameters over a range of temperatures for PDMS. Results for some of the probes have been omitted for clarity; the values at 90 °C are listed in Table 7. The values and trends noted here agree reasonably well with those reported⁷ at 25 °C or⁴⁴ at 60 °C. Although the plots show some temperature dependence leading to small negative values of Q_{12} , the variation is at least an order of magnitude lower the temperature dependence observed for χ and χ^* . The alkane probes yielded a comparatively narrow range of values and were

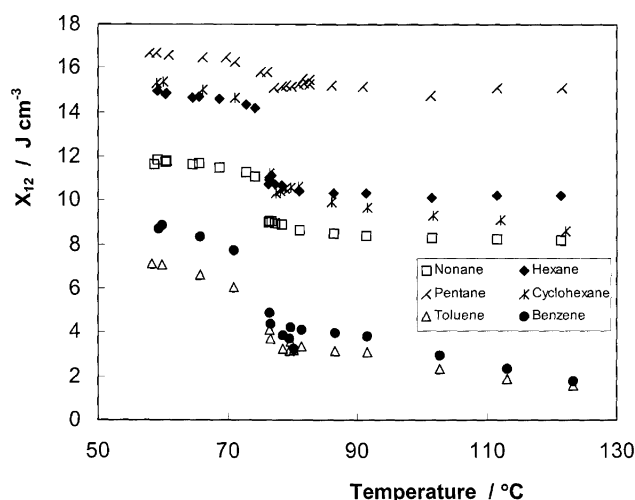


Figure 9. Energy exchange interaction parameters for probe solvents in HCB.

very small, indicating that the interactions were similar to those in the pure components. X_{12} increased somewhat with alkane chain length and decreased with branching, all following the expected trends for an energy parameter dependent on the surface area of contact. Higher values were observed for the aromatic probes, also expected given their chemical differences compared with the polymer.

The behavior of X_{12} in the LC systems is illustrated for HCB and OCB in Figures 9 and 10, respectively. Here, the temperature dependence was generally larger than in PDMS and would give positive entropy contributions to Q_{12} , the exception being the SmA phase in OCB. Both LC's exhibited clear differences between the different phases and mesophases for any given probe with values higher in the more ordered phases.

In the HCB–alkane systems, X_{12} values were significantly larger than for PDMS. As discussed above, the “true” χ^* values would be lower than those reported and it follows that X_{12} would also be lower. However, the *n*-alkane–HCB values would still be considerably higher than those reported for PDMS. The interaction between HCB and *n*-alkanes was unfavorable but became more favored as the alkane chain length increased. The higher values in the N phase are indicative of the lower flexibility of the probes in the LC mesophases.

Interactions between HCB and the aromatic probes were more favorable and there was considerable temperature dependence. The difference between nematic values and isotropic values was

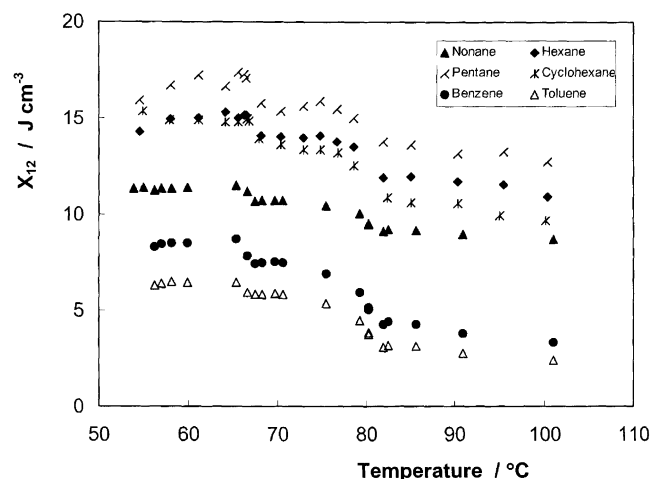


Figure 10. Energy exchange interaction parameters for probe solvents in OCB.

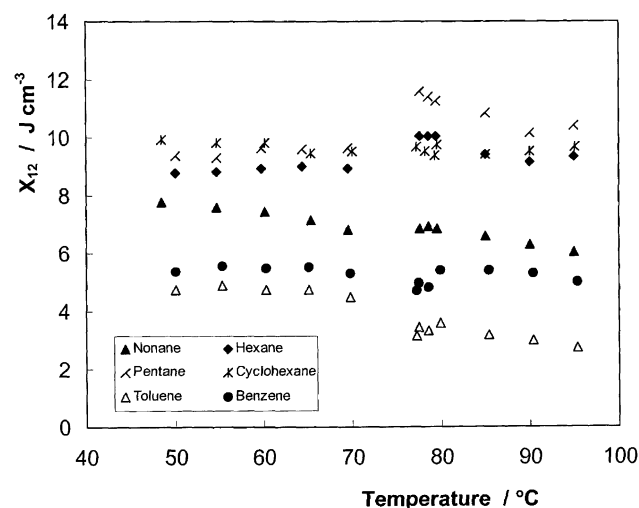


Figure 11. Energy exchange interaction parameters for probe solvents in PDCBBS.

much higher for the aromatic than aliphatic probes which indicates the preference of aliphatic probes to avoid the rigid portion of the mesogen in the mesophase. This supports our earlier conclusions that the rigid portion of the mesogen governs interaction between the liquid crystal and probe. Also, the similarity in the results for the three xylene isomers reinforces the dominance of dispersion forces on interactions in these solutions as opposed to dipolar interactions. The exchange interaction parameters for a given probe in OCB and HCB were similar, again supporting the argument that the mesogen largely governs interactions. In the smectic mesophase the values were almost constant.

Comparison of the X_{12} values in PDCBBS shown in Table 7 and Figure 11, show them to be intermediate between those of OCB and PDMS but closer to the former, again consistent with our contention that the enthalpic interactions are largely governed by the mesogen. For a given probe in the smectic mesophase of PDCBBS there was a larger temperature dependence than in OCB. In the isotropic phase, the temperature dependence of X_{12} is greater than in the smectic mesophase. The decrease in values compared to OCB could be a result of the influence of favorable interactions with the polysiloxane backbone, but the discrepancy could equally be a result of the approximations of the theory discussed above. The aromatic probes exhibit behavior similar to that observed in OCB. The

results indicate there was a contribution to the interaction from the polymer backbone. This contribution was greater in smectic mesophase than in the isotropic phase, suggesting that the mesophase is relatively inaccessible to the alkane probe. With aromatic probes, the effect was much less marked, indicating that the probe can enter the mesophase. These observations further illustrate that the rigid portion of the mesogen dominates interaction with contributions from the linking chain or backbone, only becoming significant when a probe has poor interaction with the rigid mesogen.

The equation of state model of solution behavior has allowed the interaction behavior to be discussed in terms of an enthalpic contribution and a "free-volume" contribution. Exchange interaction parameters for the liquid crystal systems imply that the enthalpic interactions are very similar for all the cyanobiphenyls studied and the differences observed in the interaction parameters arise largely from "free-volume" effects. The application of this more rigorous solution model does not alter trends in the interaction parameters between probes and the results support earlier conclusions that solution behavior is governed by the rigid mesogen and not by the flexible end groups of the liquid crystal molecule.

Conclusions

This work reports a range of parameters describing interactions at infinite dilution between cyanobiphenyl liquid crystals and nonmesogenic, nonpolar solvents. The values can be interpreted in terms of the chemical structures of the compounds involved and the various enthalpic and entropic contributions to the interactions have been determined. As far as we are aware, a detailed comparison of the thermodynamics of a low molar mass mesogen with a polymeric analogue has not previously been reported. The results show that the interactions in the LC polymer are dominated by the mesogenic group with the polymer backbone having only a minor effect. PDMS is unusual in having an extremely flexible chain and low glass transition. It would be of interest to determine whether the same effects operate in other polymer systems and this work is underway. The results reported have implications in the design of novel LC-solvent systems and for the development of new analytical chromatography phases for the separation of closely related compounds.

Acknowledgment. We are grateful to UK-EPSRC for the award of a Research Studentship (to I.M.S.) and to Merck Ltd. (Poole, U.K.) for provision of the LC materials.

References and Notes

- (1) McArdle, C. B. *Side chain liquid crystal polymers*; Blackie: London, 1989.
- (2) Chandrasekhar, S. *Liquid crystals*, 2nd ed; Cambridge University Press: Cambridge, U.K., 1992; Chapter 3.
- (3) Khoo, I. C. *Liquid crystals: physical properties and nonlinear optical phenomena*; Wiley-Interscience: New York, 1995.
- (4) *Inverse Gas Chromatography: Characterisation of Polymers and Other Materials*; Lloyd, D. R., Ward, T. C., Schreiber, H. P., Eds.; American Chemical Society: Washington, DC, 1989; Vol. 391.
- (5) Guillet, J. E.; Al-Saigh, Z. Y. *Inverse Gas Chromatography in the Analysis of Polymers*. In *Encyclopedia of Analytical Chemistry: Instrumentation and Applications*; Meyers, R., Ed.; Wiley: Chichester, U.K., 2000; Vol. 9; p 7759.
- (6) Ashworth, A. J.; Chien, C. F.; Furio, D. L.; Hooker, D. M.; Kopeck, M. M.; Laub, R. J.; Price, G. J. *Macromolecules* **1984**, *17*, 1090.
- (7) Summers, W. R.; Tewari, Y. B.; Schreiber, H. P. *Macromolecules* **1972**, *5*, 12.
- (8) Chow, L. C.; Martire, D. E. *J. Phys. Chem.* **1971**, *75*, 2005.
- (9) Oweimreen, G. A.; Lin, G. C.; Martire, D. E. *J. Phys. Chem.* **1979**, *83*, 2111.

- (10) Martire, D. E. *J. Chromatogr.* **1987**, 406, 27.
(11) Ghodbane, S.; Oweimreen, G. A.; Martire, D. E. *J. Chromatogr.* **1991**, 556, 317.
(12) Oweimreen, G. A.; AlTawfiq, A. M. *J. Chem. Eng. Data* **1997**, 42, 996.
(13) Martire, D. E.; Yan, C. *Anal. Chem.* **1992**, 64, 1246.
(14) Bocquet, J. F.; Pommier, C. *J. Chromatogr.* **1983**, 261, 11.
(15) Coca, J.; Medina, I.; Langer, S. H. *Chromatographia* **1988**, 25, 825.
(16) Maier, W.; Saupe, A. Z. *Naturforsch.* **1960**, 15, 287.
(17) Lee, Y. S.; Bae, Y. C. *J. Polym. Sci., Part A: Polym. Chem.* **2000**, 38, 4128.
(18) Benmouna, F.; Maschke, U.; Coqueret, X.; Benmouna, M. *Macromol. Theory Simul.* **2000**, 9, 215.
(19) Laub, R. J. Reference 4, Chapter 14.
(20) Price, G. J.; Shillcock, I. M. *Polymer* **1993**, 34, 85.
(21) Romansky, M.; Smith, P. F.; Guillet, J. E.; Griffin, A. C. *Macromolecules* **1994**, 27, 6297.
(22) Tovar, G.; Carreau, P. J.; Schreiber, H. P. *Colloids Surf. A* **2000**, 161, 213.
(23) Price, G. J.; Shillcock, I. M. *Phys. Chem. Chem. Phys.* **2002**, 4, 5307.
(24) Schuld, N.; Wolf, B. A. *J. Polym. Sci., Polym. Phys.* **2001**, 39, 651.
(25) Petri, H. M.; Schuld, N.; Wolf, B. A. *Macromolecules* **1995**, 28, 4975.
(26) Eichinger, B. E.; Flory, P. J. *Trans. Faraday Soc.* **1968**, 64, 2035.
(27) Flory, P. J. *Discuss. Faraday Soc.* **1970**, 49, 7.
(28) Martire, D. E.; Yan, C. *J. Phys. Chem.* **1992**, 96, 7510.
(29) Jonah, D. A.; Brostow, W.; M.; H. *Macromolecules* **1993**, 26, 76.
(30) Blonski, S.; Brostow, W.; Jonah, D. A.; Hess, M. *Macromolecules* **1993**, 26, 84.
(31) Flory, P. J.; Ronca, G. *Mol. Cryst. Liq. Cryst.* **1979**, 54, 289.
(32) Flory, P. J.; Irvine, P. A. *J. Chem. Soc., Faraday Trans. 1* **1984**, 80, 1807.
(33) Flory, P. J. *Macromolecules* **1969**, 1, 285.
(34) Price, F. P.; Fritzche, A. K. *J. Phys. Chem.* **1973**, 77, 396.
(35) Conder, J. R.; Young, C. L. *Physicochemical measurement by gas chromatography*; Wiley: New York, 1978.
(36) *Selected values of the properties of hydrocarbons and related compounds: Thermodynamics Research Centre Data Project*; Texas A&M University: College Station, TX, 1965, and later revisions.
(37) James, A. T.; Martin, A. J. P. *Biochem. J.* **1952**, 50, 679.
(38) Everett, D. H. *Trans. Faraday Soc.* **1965**, 61, 1637.
(39) McGlashan, M. L.; Potter, D. J. B. *Proc. R. Soc. London A* **1962**, 267, 478.
(40) Dymond, J. H.; Smith, E. B. *The virial coefficients of pure gases and mixtures, a critical compilation*; Clarendon Press: Oxford, U.K., 1980.
(41) Reid, R. C.; Prausnitz, J. M.; Sherwood, T. K. *The properties of gases and liquids*, 3rd ed.; McGraw-Hill: New York, 1977.
(42) Chein, C.-F.; Kopecni, M. M.; Laub, R. J.; Smith, C. A. *J. Phys. Chem.* **1981**, 85, 1864.
(43) Lichtenthaler, R. N.; Liu, D. D.; Prausnitz, J. M. *Ber. Bunsen-Ges. Phys. Chem.* **1974**, 78, 470.
(44) Galin, M. *Macromolecules* **1977**, 10, 1241.
(45) Roth, M.; Novak, J. *Macromolecules* **1986**, 19, 364.
(46) Matheson, R. R.; Flory, P. J. *Macromolecules* **1981**, 14, 954.
(47) Price, G. J.; Shillcock, I. M. *Can. J. Chem.* **1995**, 73, 1883.
(48) Flory, P. J.; Abe, A. *Macromolecules* **1978**, 11, 1119.